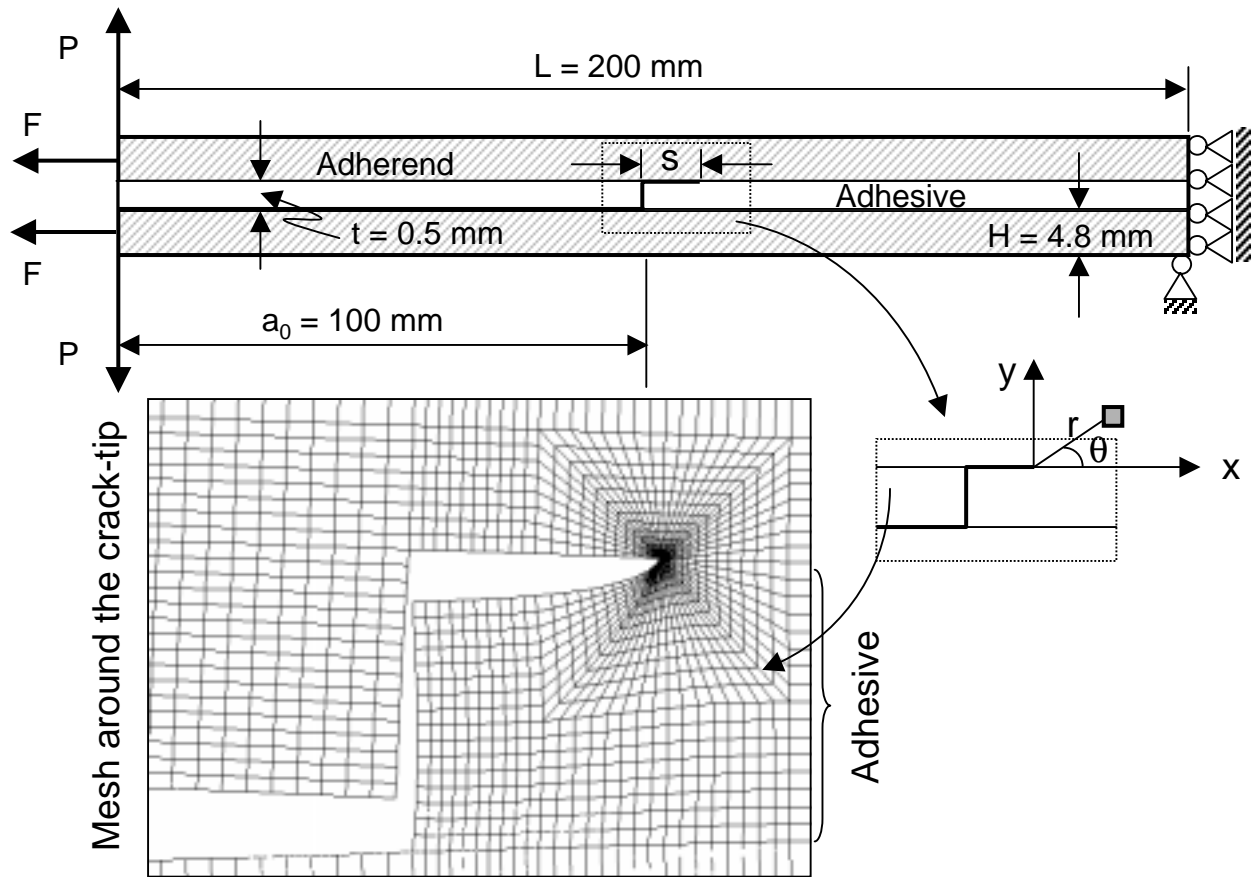
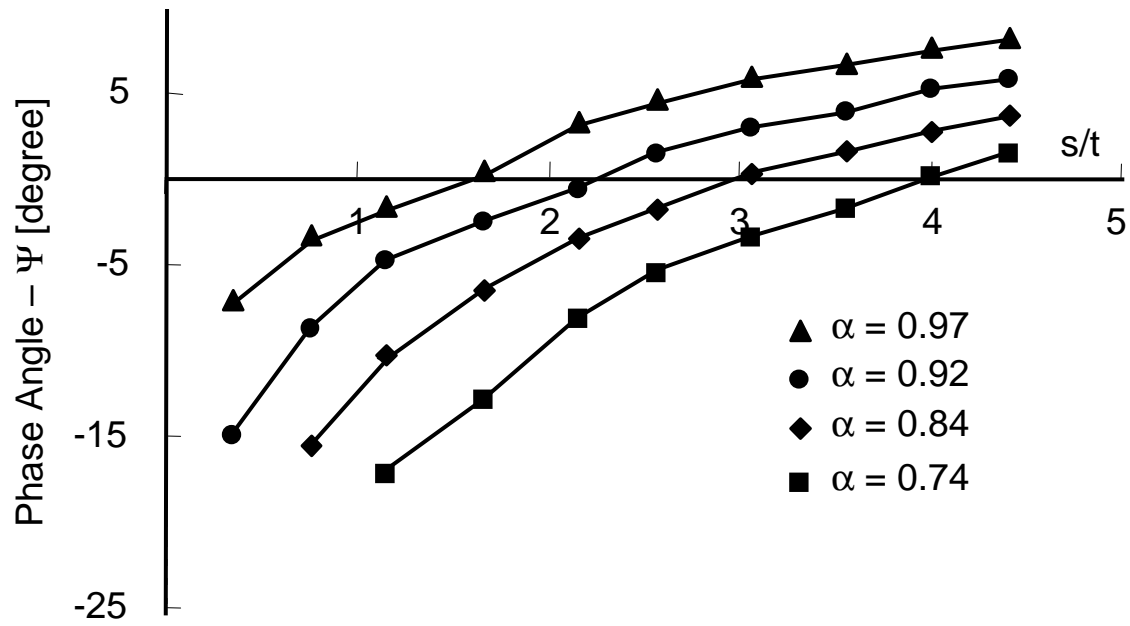


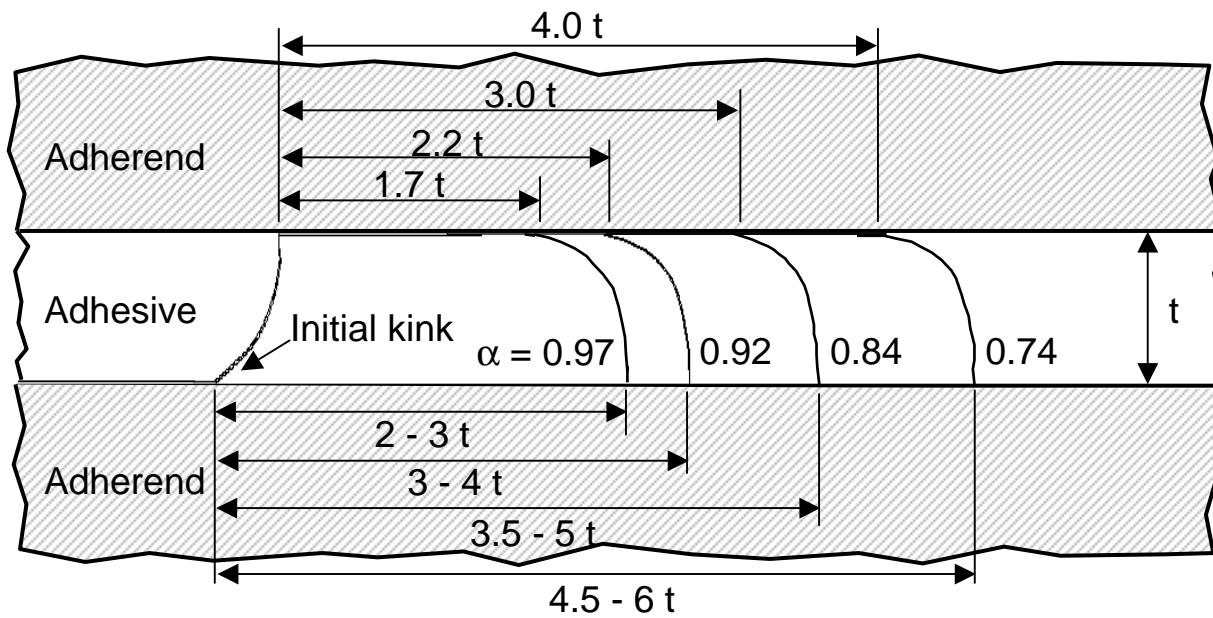
**Fig. 1.** The directional stability of cracks in DCB specimens predicted using the energy balance model in reference [12]. The strain energy available is normalized to  $G_c = 310 \text{ J/m}^2$



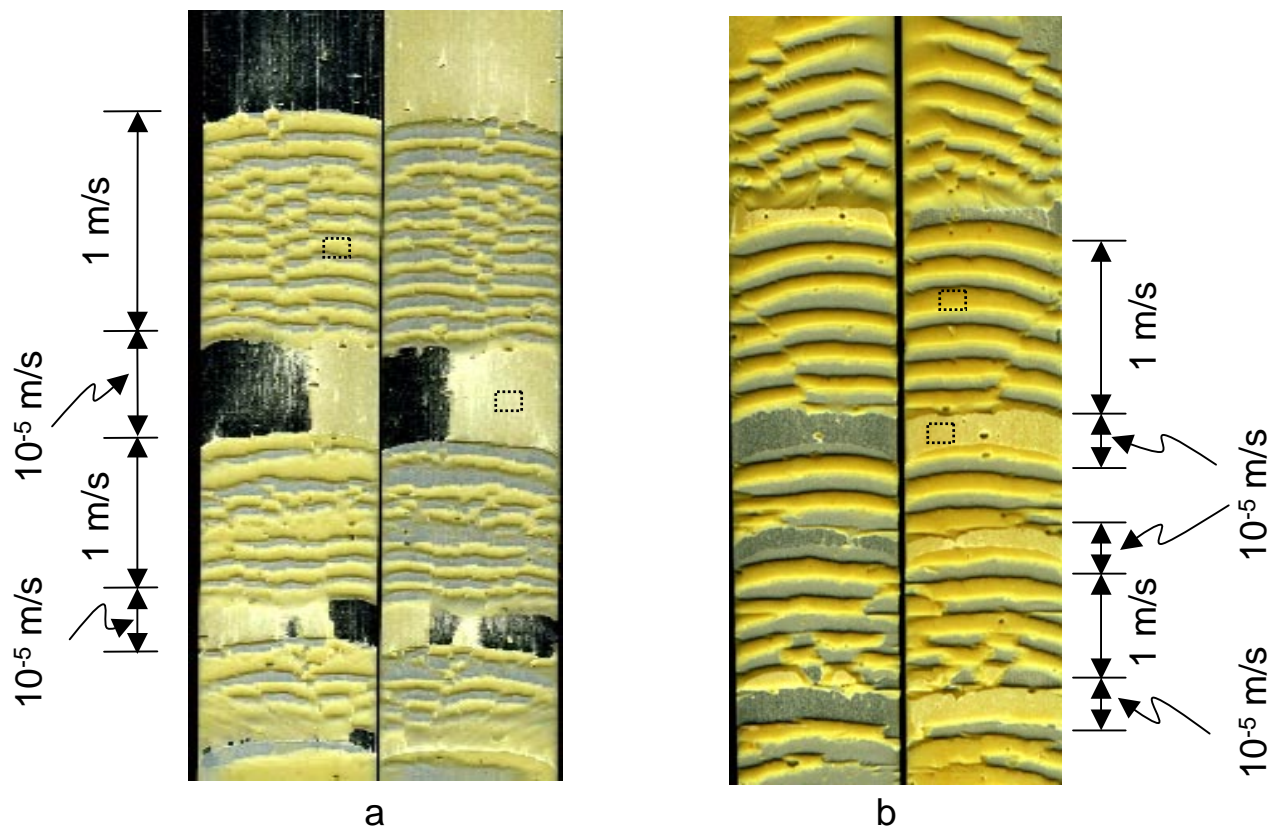
**Fig. 2.** The DCB specimen geometry used in the finite element analysis to determine the crack propagation behavior after the kinking occurred. The insert is the mesh around the crack-tip.



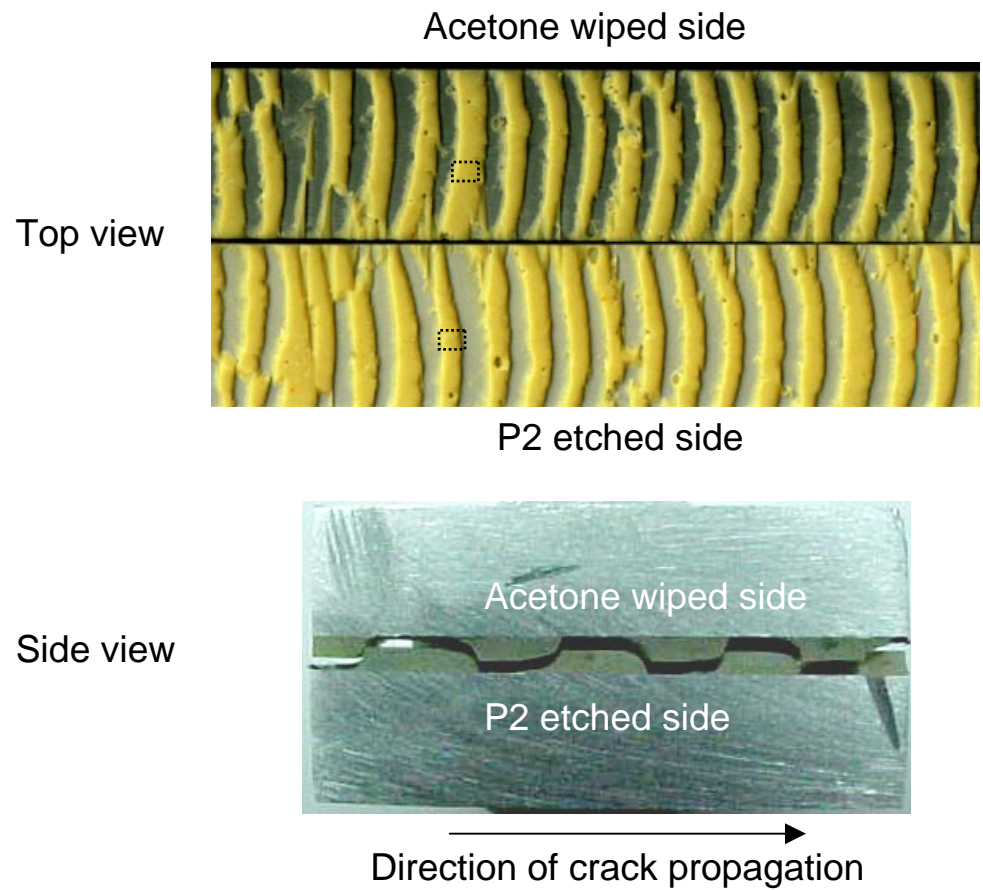
**Fig. 3.** The phase angle at the crack tip versus the normalized kinked crack length  $s/t$  for different materials combinations obtained from the parametric study.




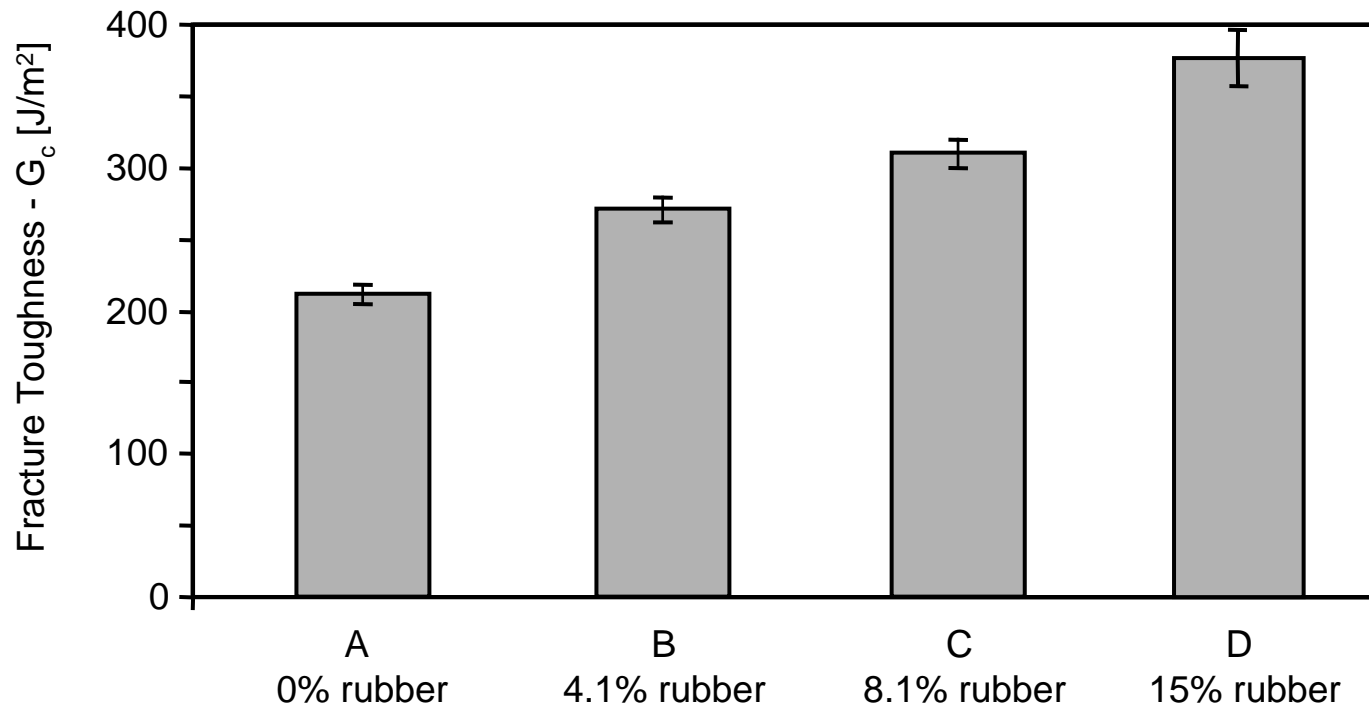
**Fig. 4.** The crack trajectories of directionally unstable crack propagation for different materials systems predicted using the finite element analysis.



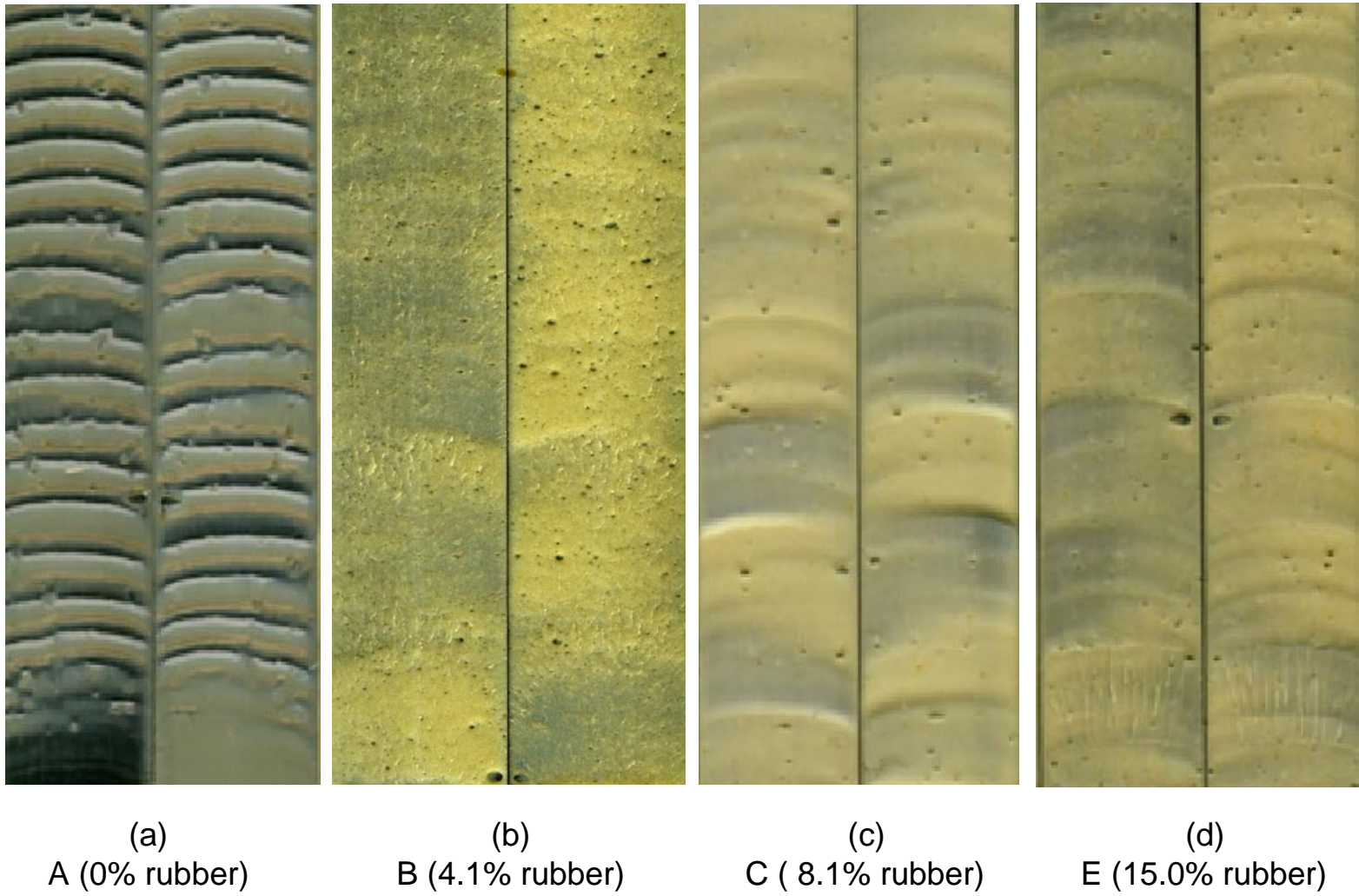
**Fig. 5.** The failure surfaces of the DCB specimens prepared using acetone wipe (a) and P2 etch (b), respectively. The  $\square$  indicates the areas where XPS analyses were conducted.



**Fig. 6.** The failure surfaces and the crack trajectory of the DCB specimen with asymmetric surface preparation. The  indicates the areas where XPS and Auger analyses were conducted.

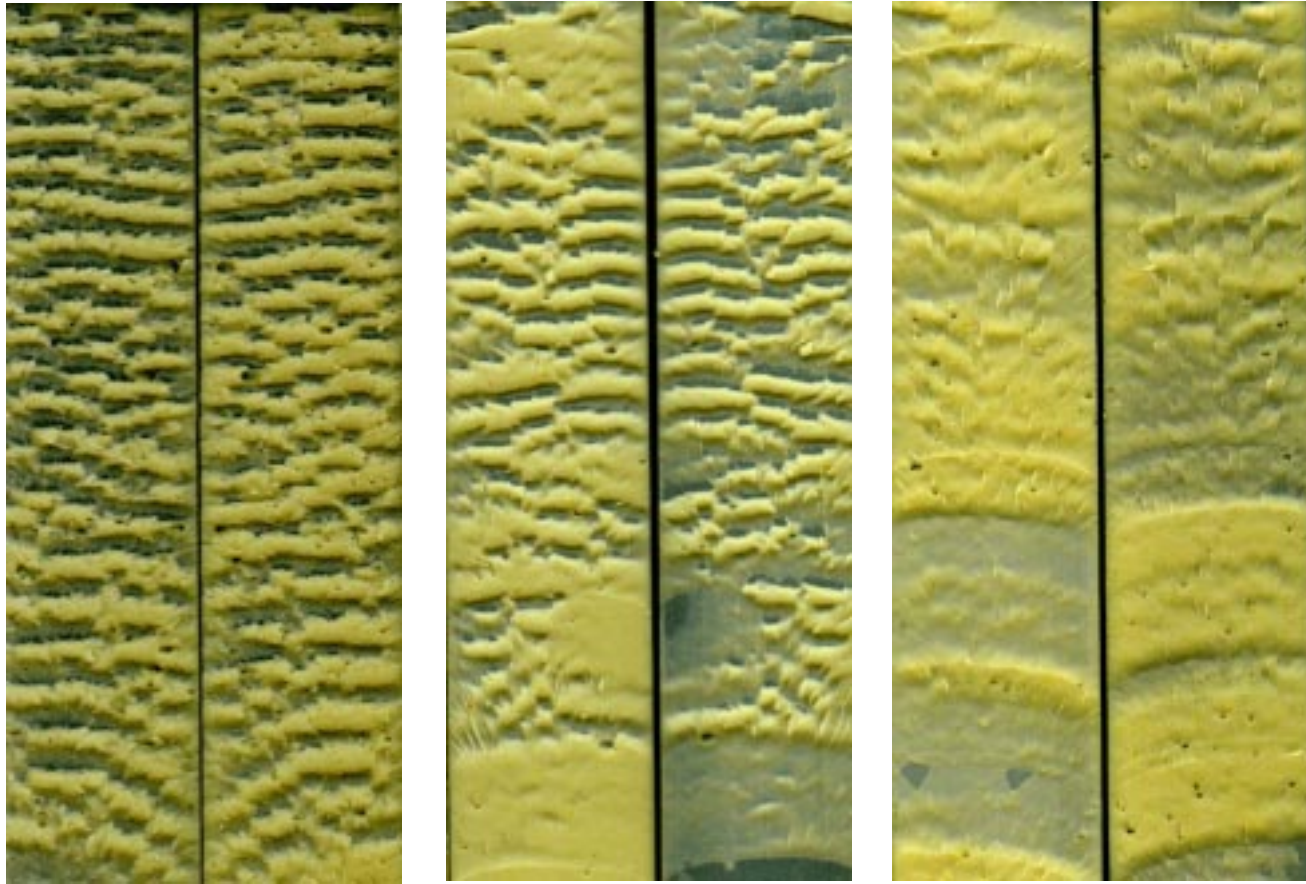


**Fig. 7.** The fracture toughness of the DCB specimens using adhesives with different levels of rubber concentrations. Error bars represent  $\pm 1$  standard deviation.



**Fig. 8.** The failure surfaces of the as-produced DCB specimens prepared using different adhesives.





(a)  
B (4.1% rubber)

(b)  
C (8.1% rubber)

(c)  
E (15.0% rubber)

**Fig. 9.** The failure surfaces of the DCB specimens prepared using different adhesives. All the specimens contained 1.1% plastic deformation in the adherends